Title
An Energy Dispersive X-ray Fluorescence (EDXRF) Analysis of Obsidian Artifacts from Three Prehistoric Sites near Darwin, Inyo County, California

Author
Shackley, M. Steven

Publication Date
1993-02-23

AN ENERGY DISPERSIVE X-RAY FLUORESCENCE (EDXRF) ANALYSIS OF OBSIDIAN ARTIFACTS FROM THREE PREHISTORIC SITES NEAR DARWIN, INYO COUNTY, CALIFORNIA

by

M. Steven Shackley

Phoebe Hearst Museum of Anthropology
University of California, Berkeley

Report Prepared for

Ancient Enterprises, Inc.

Santa Monica, California

23 February 1993

INTRODUCTION

The following is a report of a x-ray fluorescence analysis of 39 obsidian artifacts recovered from three prehistoric sites in Inyo County (CA-Iny-2844, 2845, 2847). All 39 specimens were derived from one of the chemical source localities in the Coso Volcanic Field in Inyo County, California.

ANALYSIS AND INSTRUMENTATION

All samples were analyzed whole, and were washed in distilled water before analysis. The results presented here are quantitative in that they are derived from "filtered" intensity values ratioed to the appropriate x-ray continuum regions through a least squares fitting formula rather than plotting the proportions of the net intensities in a ternary system (McCarthy and Schamber 1981; Schamber 1977). Or more essentially, these data through the analysis of international rock standards, allow for inter-instrument comparison with a predictable degree of certainty (Hampel 1984).

The trace element analyses were performed in the Department of Geology and Geophysics, University of California, Berkeley, using a Spectrace 440 (United Scientific Corporation) energy dispersive x-ray fluorescence spectrometer. The spectrometer is equipped with a Rh x-ray tube, a 50 kV x-ray generator, with a Tracor X-ray (Spectrace) TX 6100 x-ray analyzer using an IBM PC based microprocessor and Tracor reduction software. The x-ray tube was operated at 30 kV, .20 mA, using a .127 mm Rh primary beam filter in a vacuum path at 250 seconds livetime to generate x-ray intensity Kα-line data for elements titanium (Ti), manganese (Mn), iron (as Fe^T), rubidium (Rb), strontium (Sr), yttrium (Y), zirconium (Zr), and niobium (Nb). Weight percent iron ($Fe=Fe_2O_3{}^T$) can be derived by multiplying ppm estimates by 1.431 (Glascock 1991). Trace element intensities were converted to concentration estimates by employing a least-squares calibration line established for each element from the analysis of up to 26 international rock standards certified by the U.S. Bureau of Standards, the U.S. Geological Survey, Canadian

Centre for Mineral and Energy Technology, and the Centre de Recherches Pétrographiques et Géochimiques in France (Govindaraju 1989). Further details concerning the petrological choice of these elements in Southwest obsidians is available in Shackley (1988, 1990; also Mahood and Stimac 1991).

The data from the Tracor software were translated directly into Quattro Pro 4.0 software for manipulation and on into SPSSPC+ 3.0 for statistical analyses. In order to evaluate these quantitative determinations, machine data were compared to measurements of known standards. Table 1 shows a comparison between values recommended for two international rock standards, one rhyolite (RGM-1) and one obsidian (NBS-278). One of these standards is analyzed during each sample run to insure continued machine calibration. The results shown in Table 1 indicate that the machine accuracy is quite high, and comparable to Hughes (1988) analysis of Coso source material..

Trace element data exhibited in Tables 1 and 2 are reported in parts per million (ppm), a quantitative measure by weight. Source probability is based on a comparison with 1-sigma level of variability. Table 2 exhibits the trace element concentrations for the 39 samples. Source standard data for the Coso glass can be found in Hughes (1988). Figures 1 through 4 display bivariate plots of the data using five elements.

DISCUSSION

Not unexpectedly, all the material was derived from one of the obsidian procurement areas in the Coso Volcanic Field. Hughes (1988) feels confident that the various events can be distinguished through XRF analyses, but Bouey (1991) disputes this assumption suggesting that the range of variability detected by Hughes is typical of large rhyolite glass extrusions. There is some variability within the analyzed sample here. Samples 632156 and 633S79 both exhibit larger concentrations of manganese, but the remaining elements fit within the Coso geochemical range. Additionally, the caliche on some of the specimens may also influence the analyzed chemistry.

In most cases, the problem of intra-source variability is not significant for archaeological research since the distance to the source is essentially the same. The dominance of Coso glass at these three sites is a reflection of the proximity to this excellent raw material.

REFERENCES CITED

Bouey, Paul D.
1991 Recognizing the Limits of Archaeological Applications of Non-Destructive Energy-Dispersive X-ray Fluorescence Analysis of Obsidians. In *Materials Issues in Art and Archaeology II*, edited by P.B. Vandiver, J. Druzik, and G.S. Wheeler, pp. 309-320. Materials Research Society Symposium Proceedings 185.

Govindaraju, K.
1989 1989 Compilation of Working Values and Sample Description for 272 Geostandards. *Geostandards Newsletter* 13 (special issue).

Glascock, Michael D.
1991 *Tables for Neutron Activation Analysis (3rd edition)*. Research Reactor Facility, University of Missouri, Columbia.

Hampel, Joachim H.
1984 Technical Considerations in X-ray Fluorescence Analysis of Obsidian. In *Obsidian Studies in the Great Basin*, edited by R.E. Hughes, pp. 21-25. Contributions of the University of California Archaeological Research Facility 45. Berkeley.

Hughes, Richard E.
1988 The Coso Volcanic Field Reexamined: Implications for Obsidian Sourcing and Hydration Dating Research. *Geoarchaeology* 3(4):253-265.

Mahood, Gail A., and James A. Stimac
1990 Trace-Element Partitioning in Pantellerites and Trachytes. *Geochemica et Cosmochimica Acta* 54:2257-2276.

McCarthy, J.J., and F.H. Schamber
1981 Least-Squares Fit with Digital Filter: A Status Report. In *Energy Dispersive X-ray Spectrometry*, edited by K.F.J. Heinrich, D.E. Newbury, R.L. Myklebust, and C.E. Fiori, pp. 273-296. National Bureau of Standards Special Publication 604, Washington, D.C.

Schamber, F.H.
1977 A Modification of the Linear Least-Squares Fitting Method which Provides Continuum Suppression. In *X-ray Fluorescence Analysis of Environmental Samples*, edited by T.G. Dzubay, pp. 241-257. Ann Arbor Science Publishers.

Shackley, M. Steven
1988 Sources of Archaeological Obsidian in the Southwest: An Archaeological, Petrological, and Geochemical Study. *American Antiquity* 53(4):752-772.

1990 *Early Hunter-Gatherer Procurement Ranges in the Southwest: Evidence from Obsidian Geochemistry and Lithic Technology*. Unpublished Ph.D. dissertation, Department of Anthropology, Arizona State University, Tempe.

Table 1. X-ray fluorescence concentrations for selected trace elements of two international rock standards. ± values represent first standard deviation computations for the group of measurements. All values are in parts per million (ppm) as reported in Govindaraju (1989) and this study. RGM-1 is a U.S. Geological Survey rhyolite (obsidian) rock standard, and NBS-278 is a National Bureau of Standards obsidian standard. Element-to-Oxide conversions from Glascock (1991).

SAMPLE	Ti	Mn	Fe	Rb	Sr	Y	Zr	Nb
RGM-1 (Govindaraju 1989)	1600	279	12998	149	108	25	219	8.9
RGM-1 (this study)	1513.24±46	232.86±15	13813±59	149.58±4.05	108.03±3	22.7±.86	226.8±2	10±.28
NBS-278 (Govindaraju 1989)	1468	402	14256	127.5	63.5	41	295	n.r.[1]
NBS-278 (this study)	1405±93	365±8	15399±394	130±2	68±2	43±1.7	290±4	18±2

1 n.r = no report

Table 2. X-ray fluorescence concentrations for selected elements for obsidian artifacts from the three sites. All measurements in parts per million (ppm).

SAMPLE	Ti	Mn	Fe	Rb	Sr	Y	Zr	Nb	Source
CA-Iny-2844									
631S6	392.9	245.3	9652.7	264.4	9.5	51.7	142.7	44.2	All samples derived from the Coso Volcanic Field
631S12	476.1	275.2	9936.0	259.4	8.0	45.6	117.4	49.3	
631S16	391.0	208.2	9041.2	247.6	6.7	48.9	132.1	46.4	
631S18	402.9	235.8	9649.2	272.1	8.1	53.5	141.8	51.5	
631123	465.6	233.4	10223.5	281.4	9.1	56.9	149.5	46.9	
CA-Iny-2845									
632S5	415.0	274.1	9597.1	254.2	8.2	49.9	118.9	44.0	
632S11	827.9	539.2	9622.4	186.1	20.2	31.0	145.3	36.1	
632S35	381.0	273.4	9113.8	248.8	5.3	46.0	115.8	46.4	
632S36	412.1	238.3	9714.8	235.3	9.2	45.7	146.5	42.8	
63218	325.3	220.0	8730.8	241.0	5.2	47.2	116.0	42.0	
632120	582.6	295.5	9510.6	235.3	10.3	46.9	111.4	45.6	
632156	431.8	233.4	9690.2	257.1	4.6	46.0	115.4	40.8	
632156	4112.8	414.9	8092.8	163.9	17.5	26.3	131.2	32.4	
632157	560.7	319.3	10589.7	255.9	8.1	48.4	115.7	46.1	
632221	560.5	257.8	10555.9	283.8	10.4	50.0	142.5	49.1	
632222	435.9	233.8	10044.5	283.3	8.3	56.0	139.6	51.3	
632316	376.3	220.2	7969.8	216.2	12.5	41.3	103.4	43.7	
632323	374.9	279.2	9419.4	256.8	6.3	51.4	116.9	47.7	
632324	395.8	245.5	8934.5	238.6	7.1	46.4	108.8	42.3	
632333	541.3	247.9	10665.8	232.0	15.2	48.0	163.5	43.4	
633255	558.0	235.3	9486.6	241.8	8.8	48.1	115.8	45.4	
633233	477.2	262.0	11018.1	295.9	9.7	52.1	148.0	52.1	
633224	525.2	271.7	10866.3	289.3	10.1	55.8	147.5	50.1	
633223	631.4	283.6	10775.0	276.5	10.9	53.5	142.0	49.6	
63321	1071.7	293.9	10655.8	258.7	12.4	52.1	139.2	40.4	
633137	533.7	286.3	10218.8	253.1	7.8	50.0	112.7	45.2	
633S79	5204.8	234.8	8749.9	235.9	6.4	43.0	110.3	43.9	
CA-Iny-2847									
633S70	491.4	195.2	8671.2	227.7	6.7	45.2	102.6	41.5	
633S55	446.5	254.5	9142.7	246.0	7.6	44.7	113.9	44.6	
633S49	443.1	228.9	9905.5	281.2	7.9	53.1	142.0	51.7	
633S43	538.1	219.9	10507.1	204.7	9.3	40.7	154.6	32.8	
633S38	381.2	256.3	9094.94	238.6	6.7	45.9	111.5	48.7	
633S37	447.4	237.3	9713.21	269.1	7.5	56.4	138.8	49.2	
633S33	336.8	214.2	8271.67	221.8	7.4	45.1	111.6	40.7	
633S31	440.9	208.4	8951.52	252.1	9.3	51.1	139.0	45.2	
633S23	480.9	192.5	8483.11	240.7	8.4	46.2	132.2	43.0	
633S16	752.8	228.9	8810.90	237.9	4.5	46.5	113.5	50.0	
633S5	442.6	247.2	10147.8	236.5	9.1	48.0	142.1	46.7	
633S4	527.2	231.3	10718.2	240.4	13.8	46.0	157.7	42.2	

Figure 1. Y versus Z concentration plot for obsidian artifacts from the three sites.

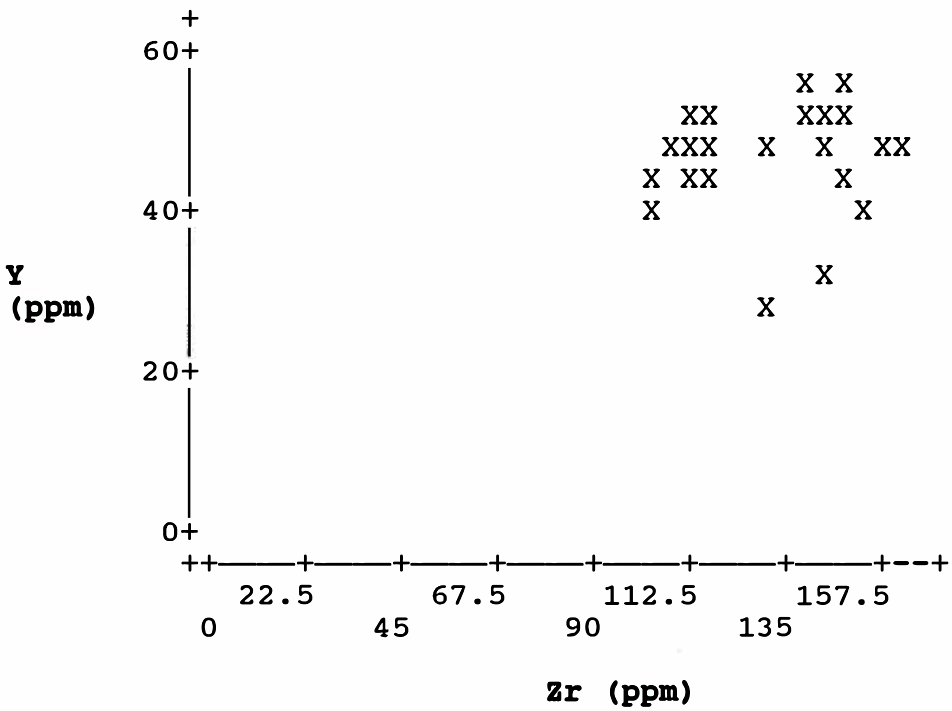

Figure 2. Rb versus Sr concentration plot for obsidian artifacts from the three sites.

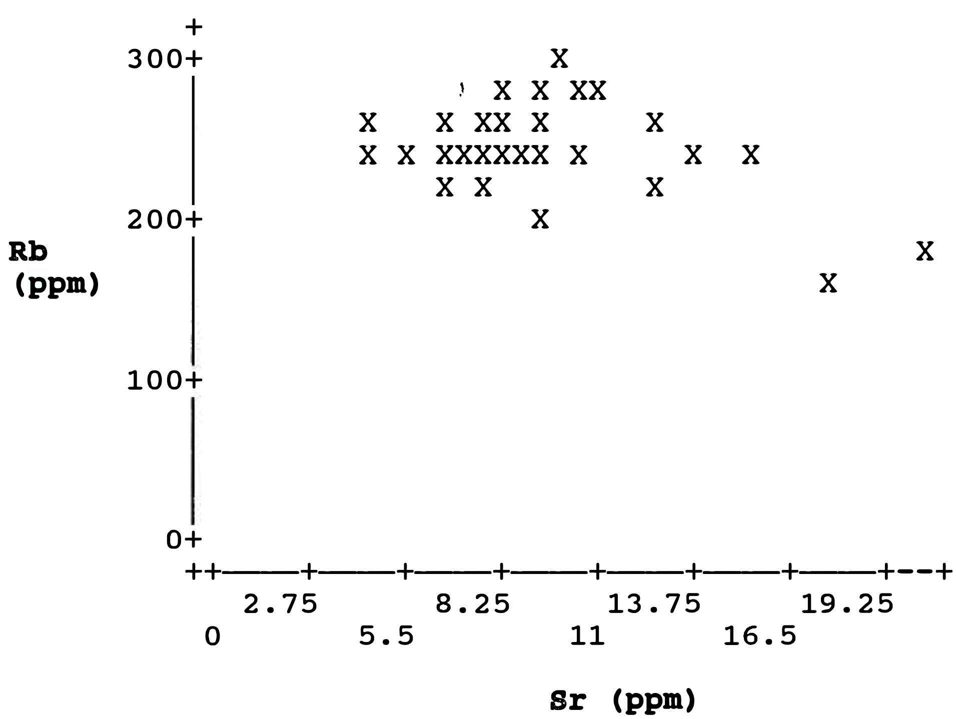

Figure 3. Mn versus Sr concentration plot for obsidian artifacts from the three sites.

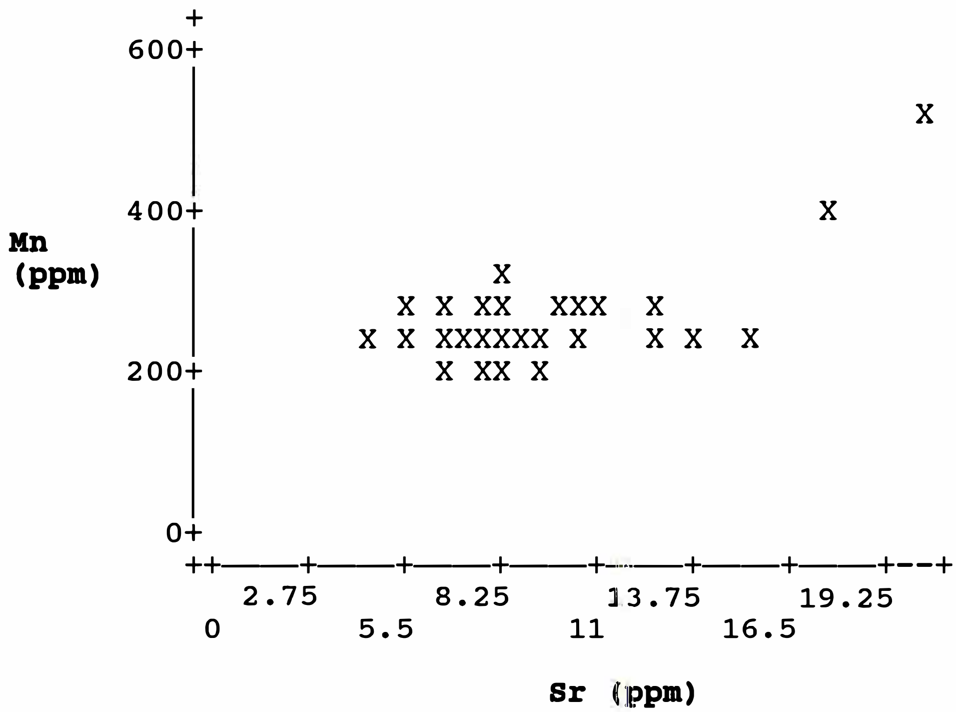

Figure 4. Rb versus Zr concentration plot for obsidian artifacts from the three sites.